Feature Article

Study of High Definition Full Color Imaging To Plain Paper by Thermal Transfer Printing*

Ikuo Hibino▲
Alps Electric Co., Ltd. Tokyo, Japan

We have analyzed the thermal transfer printing process and 600 dpi high definition thermal transfer ink ribbons. The results of our analysis revealed that four factors would play an important role in high definition thermal transfer ink ribbons: (1) the rupture strength of the ink under printing pressure and temperature, (2) the adhesive strength between the ink and paper, (3) thickness of the ink layer and (4) the adhesive strength between the heated ink and the base film. We have used a quantitative model for the printing process to design an improved ink ribbon, and we describe measurements of the viscoelastic characteristics which were used to optimize the ink materials. The improved 600 dpi high definition full color thermal transfer ink ribbon has a base of 2.5 µm polyethylene terephthalate (PET). The ink comprises two layers; a 1.3 µm ethylene-vinyl acetate copolymer thermoplastic resin and a release layer of 0.9 µm wax.

Journal of Imaging Science and Technology 47: 379-387 (2003)

Introduction

The origin of the thermal printer is relatively recent and can be dated to an idea by Joice around 1967. Figure 1 shows the development of printer technology and in particular some of the key developments in thermal transfer printer technology. Research in Japan began approximately 20 years ago by Tokunaga at the then Nippon Telegraph and Telephone Corporation. Our research began around 17 years ago. During this time the thermal printer was being utilized in over 85% of Japanese word processors, and advances in technology were being achieved. Based on our research, in 1995 the Micro Dry™ printer was introduced and drew keen attention. This printer is capable of printing full color images on plain paper. Figure 2 shows the process of thermal transfer printing. In this technology the paper and ink ribbon are tightly sandwiched between the thermal print head and the platen. The application of heat by the thermal print head melts the ink in accordance with the print signal. The ink rapidly cools below the melting temperature and the paper and ribbon are separated. In regions were the ink was melted it adheres to the paper and releases from the ink ribbon. In the standard application the ink comprises pigment in a wax binder. The left side of Fig. 3 shows how the wax-based ink transfers to papers with matte or smooth surfaces. Thus, with a rough surface the ink only transfers to the "high" spots leaving unprinted voids. In addition, the ink can be absorbed into the paper. These characteristics degrade print quality. We have developed an ink based on thermoplastic resin binders, and the right side of Fig. 3 shows that the transfer is improved.

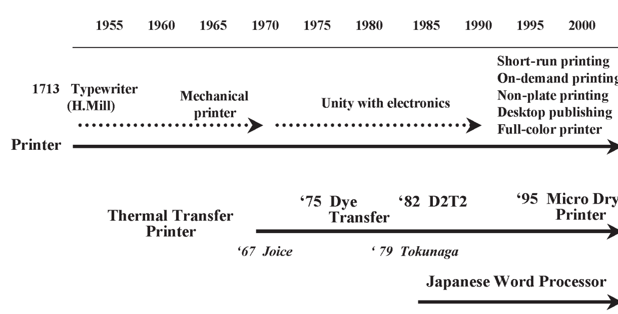

Figure 1. Historical developments in printing technologies as they relate to thermal transfer printing.

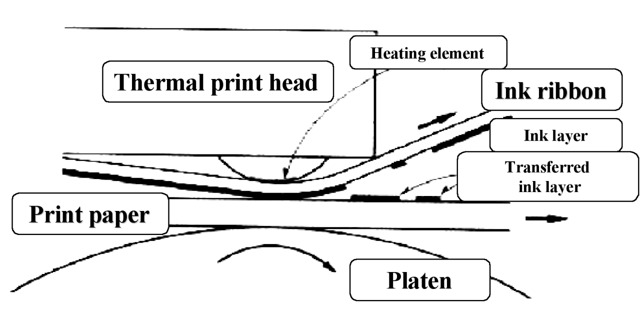

Figure 2. The thermal transfer printing process.

Original manuscript received December 3, 2002

▲ IS&T Member

*Presented in part as the Award Address for IS&T's 2002 Kosar Memorial Award.

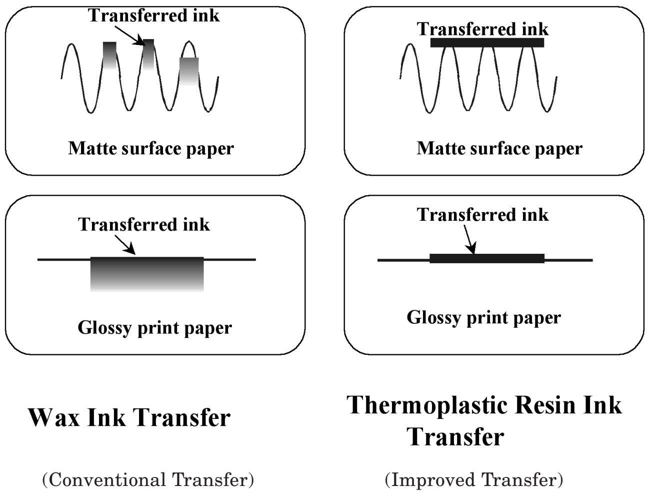

Figure 3. Ink transfer to a rough surface with the standard wax ink and with the new thermoplastic resin-based ink described in this paper.

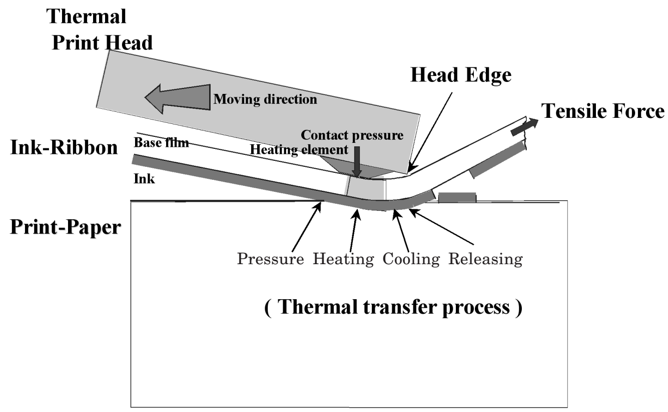

Figure 4. Elements and forces considered in our modeling of the ink transfer process.

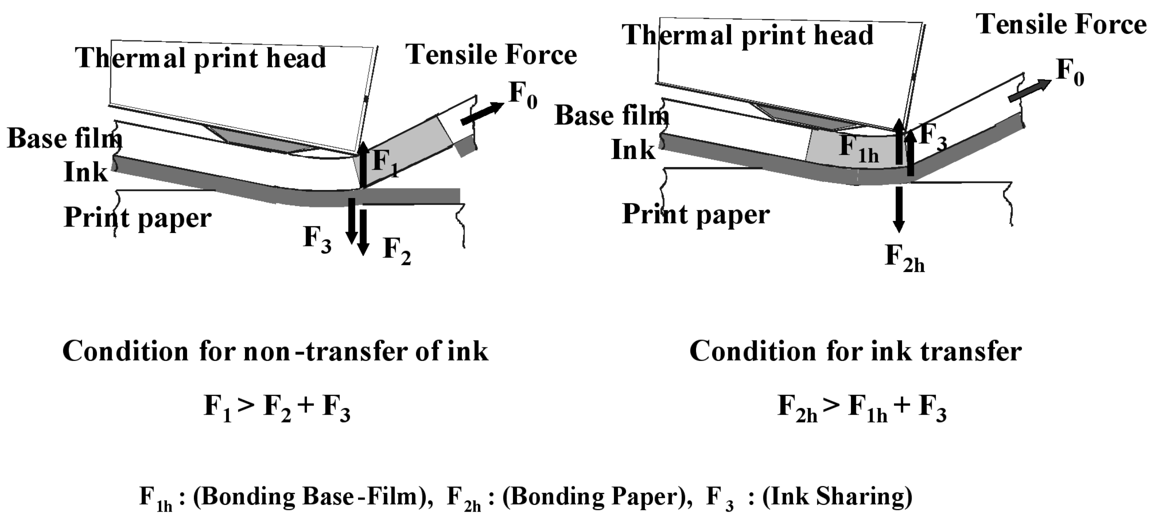

Figure 5. Dynamic model of thermal ink transfer

In this article we describe a model for thermal transfer, we show how the application of the model has led to the development of the new ink ribbon comprising a thermoplastic resin ink in a multilayer structure. We describe and characterize our new ribbon and we demonstrate its application in full color imaging on plain paper.

Thermal Ink Transfer Model

To study the process of thermal printing it was necessary to construct an engineering model of the process and to use this model to analyze the interplay of forces in the transfer of ink to paper. Figure 4 depicts an enlarged cross section of the ink transfer process. The heating element of the thermal print head contacts the back of the ink ribbon such that the ink makes contact with the paper. The diagram depicts the print paper and ribbon as being static and the thermal head as moving as shown by the arrow. The ink ribbon is composed of ink coated on a base film. The trailing edge of the thermal head is designed to contact the back of the ribbon to facilitate the release of ink from the base film to the paper.

As the thermal transfer process diagram depicts, four processes are employed: pressure, heating, cooling, and ink release. The ink transfer conditions are determined by the relationships between the ribbon tension and bonding and stress limits of the materials in the ink release process.

Figures 5 and 6 illustrate the application of this model to different configurations of the inking ribbon. In Fig. 5 the comparison is between transfer and non-transfer using a standard ink (single layer) ribbon. The dynamic model for ink transfer or non-transfer involves the relationship between three forces of delamination. The three forces of delamination are: F_1, the bonding force of delamination for ink release from the base film, F_2, the force of delamination for transfer of the ink to the paper, and F_3, the force of delamination for shearing the ink from the film base. The subscript h is used to represent cases where heating has occurred. The left chart shows the condition when the ink does not transfer. The condition for non-transfer of ink is $F_1 > F_2 + F_3$. The right chart shows the ink transfer condition when transforming from a non-transferable state to a transferable

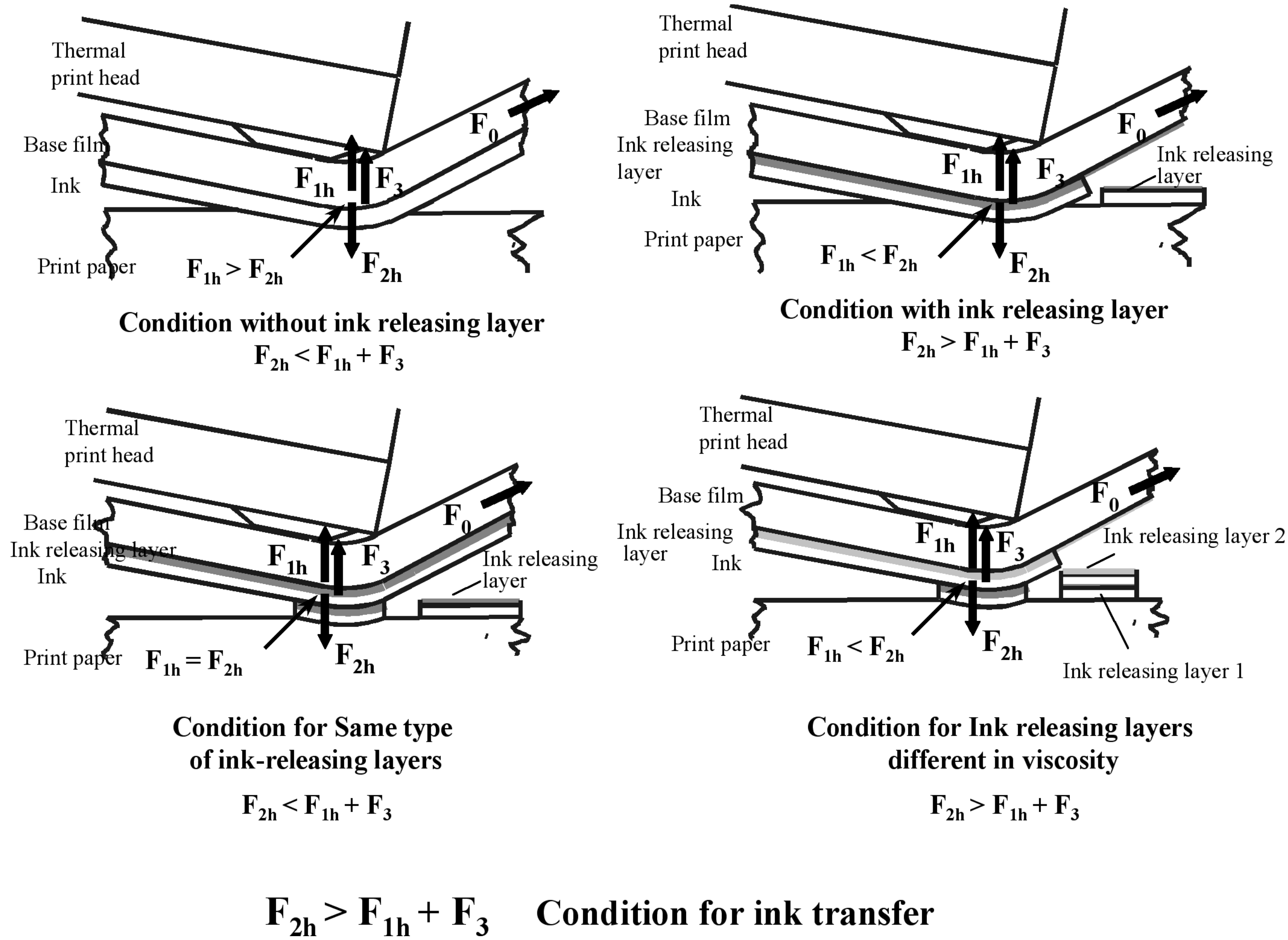

Figure 6. Comparisons of the conditions for ink transfer and non transfer depending on the structure and composition of the ink ribbon.

state. The condition for transfer of ink is $F_{2h} > F_{1h} + F_3$. The ink shearing force F_3 works in the opposite direction to ink transfer movement.

The upper side of Fig. 6 shows the conditions for thermoplastic resin ink transfer for the thermoplastic resin base single layer ink and for the improved ink ribbon which has a wax based release layer between the ink and the base film. In order to transfer the ink without being adversely effected by the surface roughness of the paper, a thermoplastic resin ink transfer is required. The diagram on the right shows the transfer conditions and limitations for a thermoplastic resin ink with a release layer. The diagram on the left depicts the process with for a single thermoplastic resin ink layer. In the case of a single layer, the side of the layer in contact with the paper is compressed more than the side where the ink is in contact with the base film, thus $F_{1\mathrm{h}} > F_{2\mathrm{h}}$. Therefore, the condition for transfer is not met because $F_{2\mathrm{h}} < F_{1\mathrm{h}} + F_3$. On the other hand, with the addition of a release layer between the ink and the base the base film bonding limit is decreased, and the condition of $F_{2\mathrm{h}} > F_{1\mathrm{h}} + F_3$ is met.

The lower side of Fig. 6 shows the transfer conditions and limitations when a double ink layer is used in a lamination transfer. The diagram on the left is the previously described double ink lamination transfer. In this case, the bonding force at the delamination limit on the base side of the laminated ink and the bonding force at the delamination limit on the paper side are the same. When $F_{1\mathrm{h}} = F_{2\mathrm{h}}$ the ink release condition is not met. However, with the addition of a release layer $F_{2\mathrm{h}} > F_{1\mathrm{h}}$ and ink transfer occurs. The diagram on the right shows the method developed in our research to solve this problem. By reducing the bonding force at the delamination limit of the ink and base film, $F_{1\mathrm{h}} < F_{2\mathrm{h}}$ is achievable. Therefore, the condition of $F_{2\mathrm{h}} > F_{1\mathrm{h}} + F_3$ is met. In this way it is possible to print full color images by transferring ink from a ribbon composed of cyan, magenta and yellow colors.

Figure 7 shows ink transferring dynamics model in a minute area. The bonding stress level for each unit area is shown as f_1 and f_2, and the shear limit is shown as f_3. The ink block length is designated as a, and thickness by t.

$$F_{2h} > F_{1h} + F_3 \tag{1}$$

$$f_{2h} \cdot a^2 > f_{1h}\, a^2 + f_3 \cdot 4at$$

$$f_{2h} \cdot a^2 - f_{1h}\, a^2 > f_3 \cdot 4at \tag{2}$$

$$(f_{2h} - f_{1h}) \cdot a^2 > 4\, t f_3\, a$$

Therefore the condition for ink transfer is $(f_{2\mathrm{h}} - f_{1\mathrm{h}})a^2 > 4tf_3a$.[2] The left side indicates the bonding stress limit value and the right side indicates the shearing stress limit value D in Fig. 8 we plot the stress limit values as

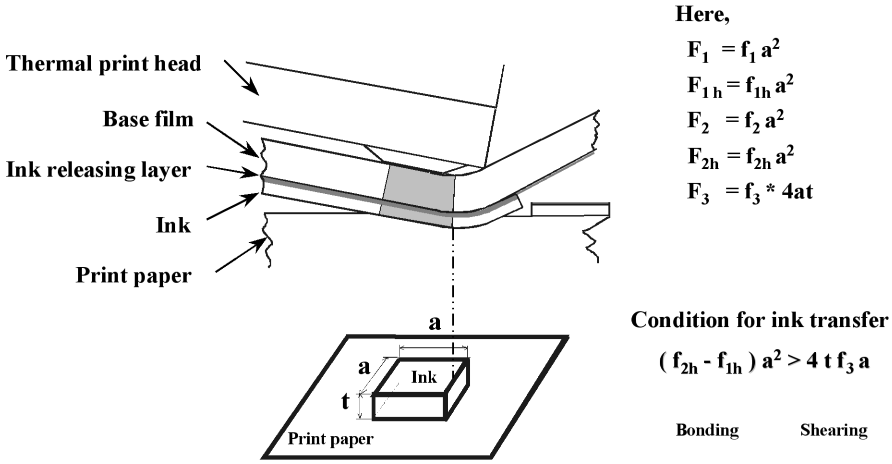

Figure 7. A model for ink transfer dynamics in a minute area.

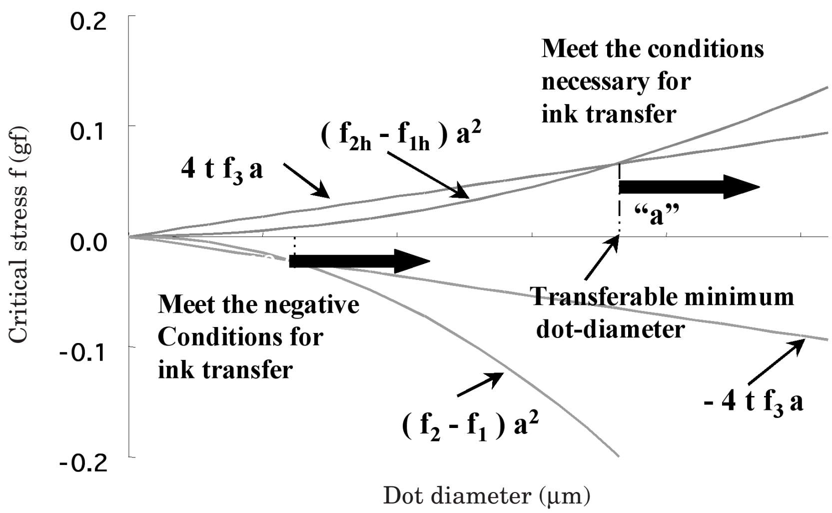

Figure 8. Prediction of the minimum transferrable dot diameter from the ink transfer model.

a function of dot diameter. The left side of the inequality is proportional to the square of a. In order to make comparison with a as shown in the graph, the minimum value of a can be obtained to meet the inequality. The minimum value of a represents the minimum dot diameter obtained in this model. The area of negative critical stress in the diagram represents non-transfer conditions. Figure 9 shows the previously derived relationship between the ink thickness and transferable minimum dot diameter. The lower the ink thickness, the smaller the lower limit of transferable dot diameter and both figures approach zero. The minimum dot size is 25 µm when the thickness of the ink layer is 2 µm.

Structure of the New Multi-layer Thermoplastic Resin Based Ink Ribbon

Figure 10 shows a cross section structure of the two layer thermoplastic resin ribbon developed from this research. It comprises a base film of 2.5 µm PET which has a heat-resistant protective layer back coat of 0.2 µm. On the base film is an ink releasing wax layer of 0.9 µm thickness and an ethylene-vinyl acetate copolymer thermoplastic resin ink layer of 1.3 µm. Full color images at 600 dpi have been printed with this ribbon.

Figure 11 shows the viscosity temperature characteristic of the thermoplastic ink used in the ribbon which we have developed. Since the thermoplastic resin is amorphous this layer undergoes a glass transition which is mirrored in the temperature dependence of viscosity as shown. As described above there is a correlation between the bonding stress limit and the viscosity of the ink such that low viscosity is desired for efficient ink transfer. The results in Fig. 11 show that this is achieved for all four colors at temperatures above approximately 85°C.

Thermal Analysis of Printing using the New Ink Ribbon

Figure 12 shows an analysis of the temperature distribution of the ink area heated in one part of a moving thermal head. The thickness of the ink is approximately 2 µm. A temperature gradient occurs from where the

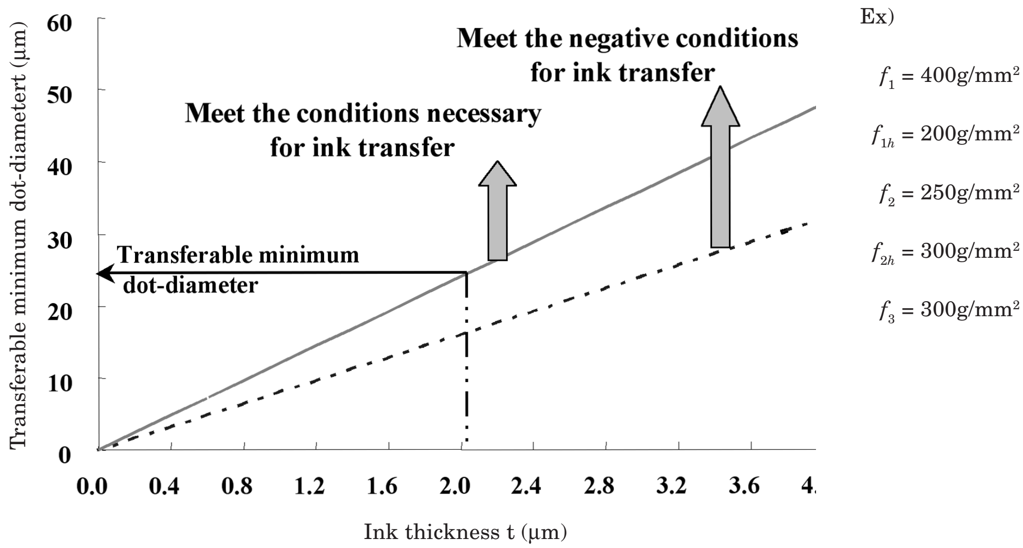

Figure 9. Relationship between the ink thickness and the minimum transferable dot diameter.

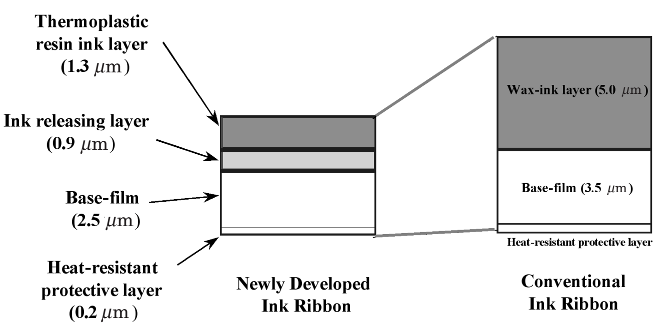

Figure 10. Vertical cross-sectional diagram of the conventional and newly developed ink ribbons.

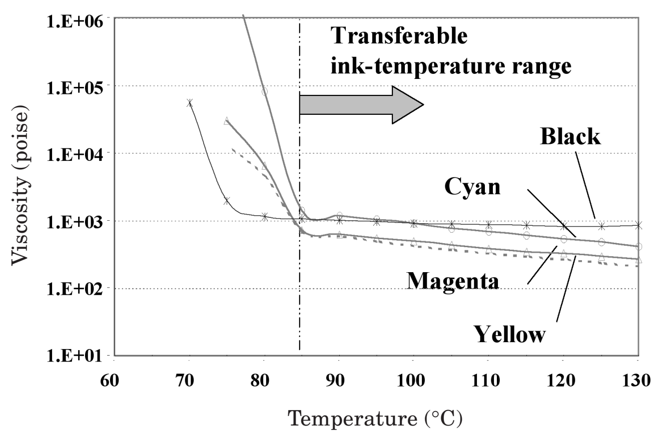

Figure 11. The temperature dependence of the viscosity of the new ink.

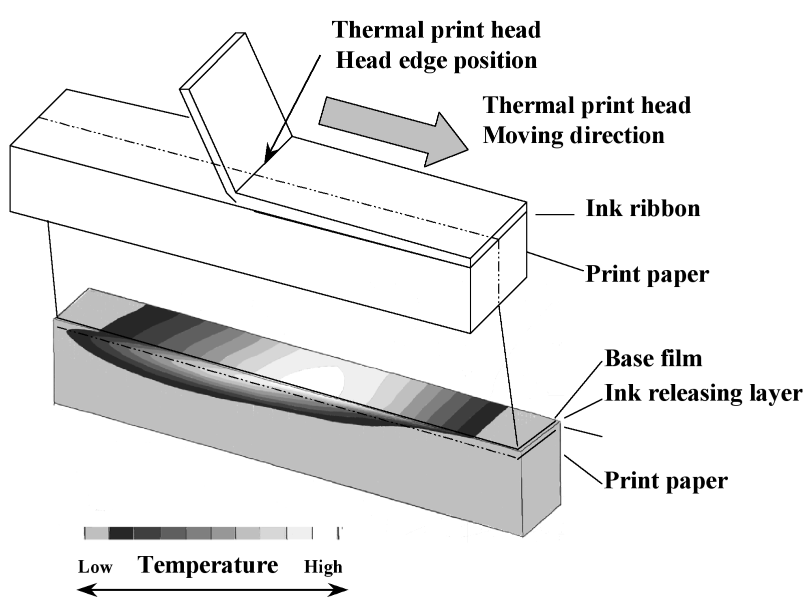

Figure 12. Temperature distribution around the ink ribbon and paper during the thermal transfer process.

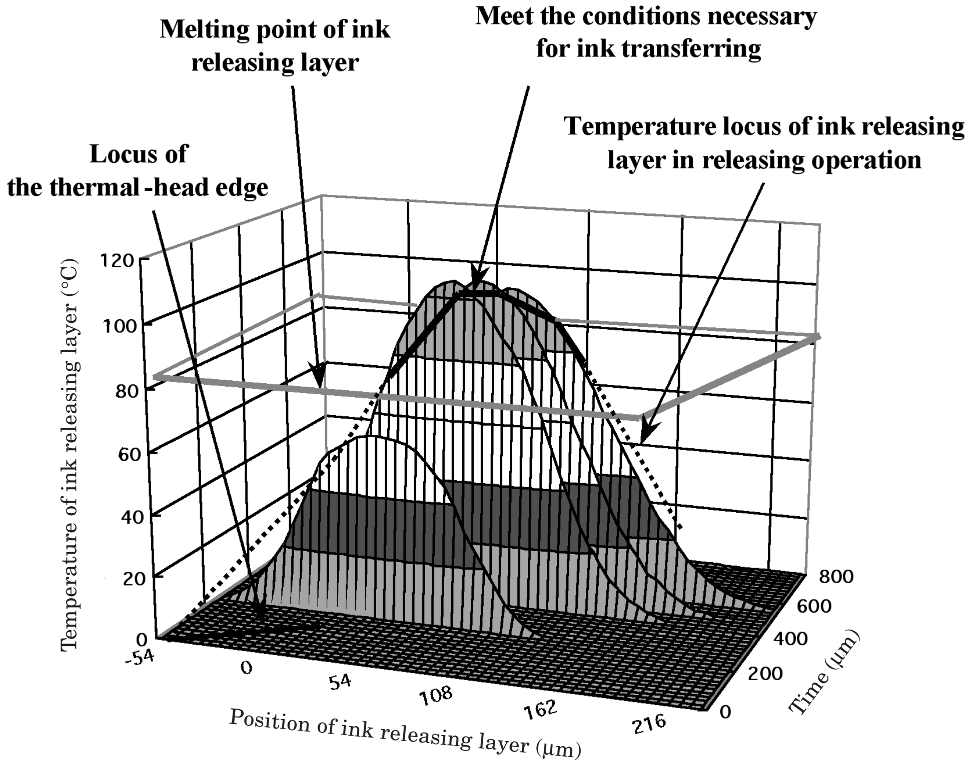

Figure 13. Temperature of the ink release layer as a function of position.

thermal head touches the back of the film base to where the ink contacts the paper, and there is a time delay from when the thermal head contacts the film base to when the paper reaches its maximum temperature. Figure 13 shows the time evolution of the ink surface temperature as a function of position in two dimensions relative to the thermal head. The plane at 85°C in the diagram is the melting point of the crystalline wax-based ink releasing layer for the ink ribbon (see Fig. 11). Above the melting point the bonding stress limit of the ink and the releasing layer material decreases greatly so the previously stated transfer conditions are realized and the possibility of transfer is achieved. The portions of the graph above the 85°C plane indicate that under these conditions the ink transfer region has a dimension about 50 μm. This is very close to the actual ink transfer value.

Evaluation of the Mechanical Properties of the New Ink Ribbon

The most important properties of thermal transfer ink are ink shear strength, adhesive strength and thermal characteristics. Many measurements have been conducted for the viscoelasticity of thermal transfer ink itself, but there have been few such measurements on ink ribbons comprising thin films of thermal transfer ink.

We have developed a method to carry out viscoelasticity measurements on our ink ribbons using a pendulum-type instrument. Such devices are generally used to measure the viscoelasticity characteristics of paint films. Pendulum-type viscoelastic instruments function by measuring oscillation damping, as shown in Fig. 14. The surface to be investigated is placed under the cylindrical fulcrum of the pendulum as shown. The elasticity and viscosity of the material influences the damping oscillation of the pendulum. The pendulum movement

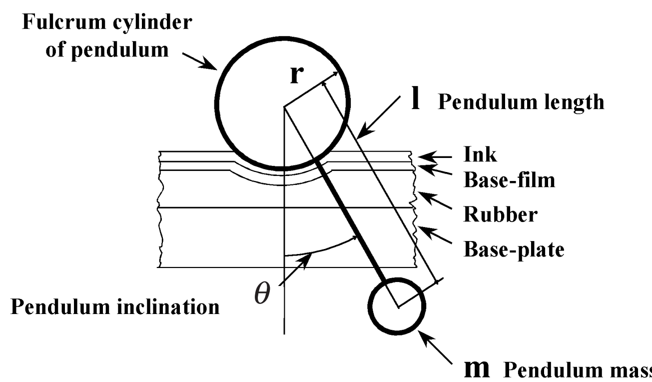

Figure 14. Diagram of the components in measuring the viscoelastic properties of an ink ribbon using the pendulum-based instrument.

is affected by the viscous damping force, which changes in relation to the velocity of the measured object. If elasticity is proportional to the displacement, the equation of motion around the cylindrical fulcrum is given as follows (Eq. 3), where θ is the angle of inclination from the perpendicular:

$$ml^2 \frac{d^2\theta}{dt^2} + C_d \frac{d\theta}{dt} + \left(mgl \sin\theta + K_d \theta\right) = 0 \qquad (3)$$

When θ is small, sin θ can be replaced with θ, then,

$$\frac{d^2\theta}{dt^2} + \frac{C_d}{ml^2}\frac{d\theta}{dt} + \left(\frac{K_d}{ml^2} + \frac{g}{l}\right)\theta = 0 \qquad (4)$$

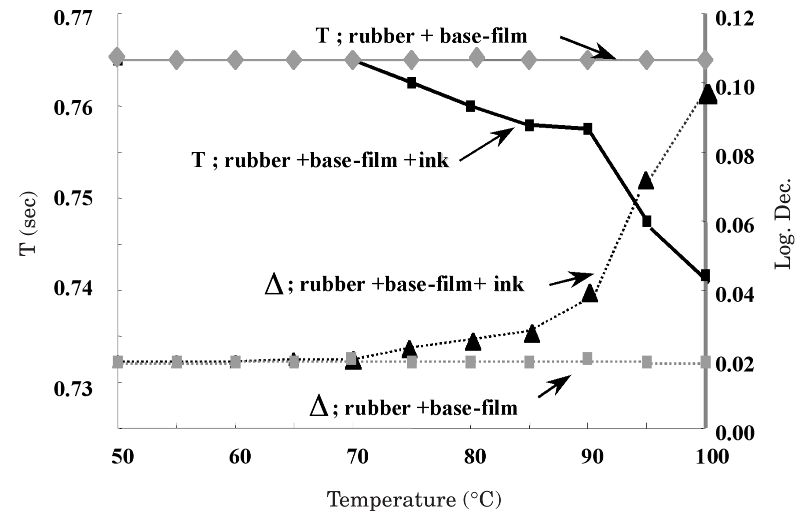

Figure 15. Oscillation cycle and logarithmic decrement-temperature properties of the high definition thermal transfer ink ribbon.

Here, m is the mass of the pendulum, l the pendulum length, g the acceleration of gravity, t is time, K_c is the elastic constant, and C_d is the viscous damping coefficient of the material under investigation. Here, we define

$$2\varepsilon = \frac{C_d}{ml^2}, n^2 = \frac{K_d}{ml^2} + \frac{g}{l} \tag{5}$$

Then Eq. 4 becomes,

$$\frac{d^2\theta}{dt^2} + 2\varepsilon\frac{d\theta}{dt} + n^2\theta = 0 \tag{6}$$

Then the logarithmic decrement is given as follows:

$$\Delta = \frac{2\pi\varepsilon}{\sqrt{\left(n^2 - \varepsilon^2\right)}} \tag{7}$$

The oscillation cycle, T, and tan δ are given as follows:

$$T = \frac{2\pi\varepsilon}{\sqrt{\left(n^2 - \varepsilon^2\right)}} \tag{8}$$

$$\tan\delta = \frac{\varepsilon}{\sqrt{\left(n^2 - \varepsilon^2\right)}} \tag{9}$$

Then,

$$C_d = 2ml^2\frac{\Delta}{T} \tag{10}$$

$$K_d = ml^2\left(n^2 - \frac{g}{l}\right) \tag{11}$$

Therefore , ε and n are given by Δ and T. And where

$$K_d = K_{d1} + K_{d2} \tag{12}$$

$$C_d = C_{d1} + C_{d2} \tag{13}$$

so that K_{d2}, C_{d2} are given by $K_d - K_{d1}$ and $C_d - C_{d1}$, respectively. Here, K_{d1} and C_{d1} represent the elastic constant and viscous damping coefficient of (Rubber + base film) respectively; K_{d2}, C_{d2} represent the elastic constant and viscous damping coefficient of ink; and K_d, C_d are the elastic constant and viscous damping coefficient of (Rubber + base film + ink) respectively.

Measurements were made on our high definition thermal transfer ink ribbon using a pendulum with a 5 mm diameter brass shaft. The ribbon sample was placed on a sample support board which was coated with 100 µm thick soft silicone rubber film. The temperature of the sample was measured with a thermocouple placed on the sample surface close to the fulcrum. Figure 15 shows the logarithmic decrement-temperature property of the ribbon. The logarithmic decrement of the soft silicone rubber, a material with low adhesiveness, is constant at around 0.03, over the temperature range. The logarithmic decrement of PET-film was 0.02 over the temperature range. PET film is harder than silicone rubber and has no adhesive characteristics. The logarithmic decrement of high definition thermal transfer ink ribbon exhibits the following characteristics: (rubber + base film) has the logarithmic decrement-temperature property of the base film; (rubber + base film + ink) has the logarithmic decrement-temperature property of the high definition thermal transfer ink ribbon. The logarithmic decrement remained constant at about 0.02 at room temperature to 60°C. From 60°C to 70°C, the logarithmic decrement increased slightly. From 70°C to 90°C, the value increased from 0.03 to 0.04. From 90°C to 100°C, the value jumped from 0.04 to 0.1.

Figure 16 illustrates the viscous damping coefficient and elastic constant-temperature property of the high definition thermal transfer ink ribbon. Ink viscosity data from Fig. 11 are also shown in this plot. These findings suggest that changes in this property corre-

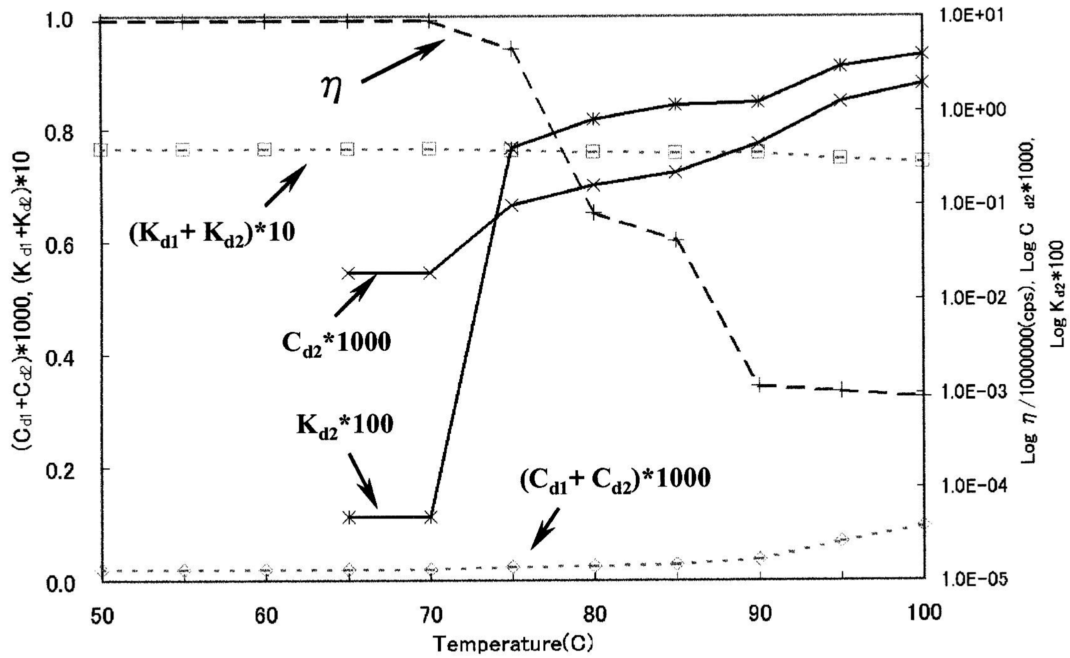

Figure 16. The viscous damping coefficient and spring constant characteristics of the high definition thermal transfer ink ribbon as a function of temperature.

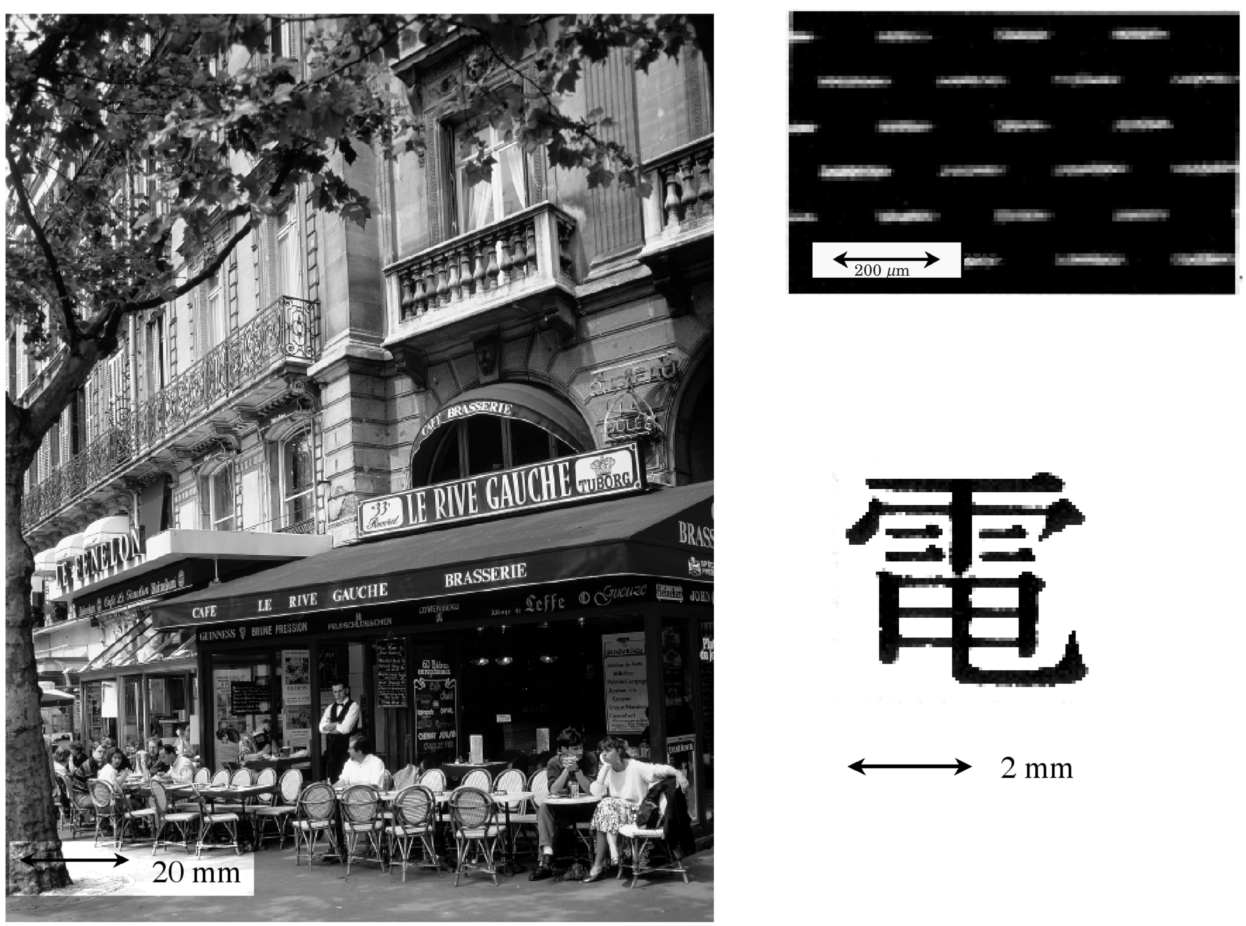

Figure 17. Printed sample using the newly developed multilayer thermoplastic resin based ink ribbon at 600 dpi.

spond to changes in the ink viscosity (see also Fig. 11). From room temperature to 70°C, both the thermoplastic resin ink layer and the wax-based ink releasing layer are solid. From 70 to 90°C, the wax layer melts. From 90 to 100°C, there is an interaction between the wax layer and the ink layer since, although the viscosity of ink decreases with the increasing temperature rise, C_d and K_d are increasing.

These results of this experiment indicate that the logarithmic decrement measured with a pendulum-type instrument does not reflect the viscoelastic characteristics of the ink material but rather the strength of the connection between the ink and the pendulum fulcrum. Therefore, we can evaluate the cohesive strength of the ink with this instrument. At some point of logarithmic decrement the ink is considered to have the required adhesive characteristics.

Figure 17 illustrates a printed sample made by high definition 600 dpi thermal transfer printing. This sample exhibits sharp, clear characters, high quality pictorial imagery, and superior light resistance. To achieve the printing density (OD value) of at least 1.5, the current pigment dispersion technology requires an ink thickness of greater than 1.3 to 1.5 μm. To reduce the thickness of the ink layer, we must increase the viscosity, thus strengthening pigment bonding. By using a thermoplastic resin as the main material for the ink layer it may be possible to satisfy this requirement for a thinner layer.

Conclusion

We inferred that the main cause of unsatisfactory print quality in traditional thermal transfer printing was because of ink voids in recessed areas of the paper and/or permeation of transferred ink into the print paper. To overcome these deficiencies we have designed a new ink ribbon which used a thermoplastic resin for the ink and had a relatively low melting wax based release layer between the ink and the substrate. In this article we have described a model for ink transfer which enabled the new design ink ribbon, as well as testing methods and results which confirm the predicted requirements for the ink ribbon characteristics. In the accomplishment of this objective we have achieved the following:

1. Constructing an ink transfer process model enabling quantitative analysis in transfer of melted ink.
2. Precise control of the thermal characteristics of the thermoplastic resin and the ink releasing layer to realize material transfer as minute dots without permeation of the paper.
3. Lowering the viscosity of the ink releasing layer which enabled transfer of the two layer ink package.
4. Precise adjustment of the thermal print head with respect to edge distance and gap to optimize transfer performance.
5. Appropriate choice of ink materials to prevent voids (lack of transfer in paper void areas) which led to enhanced print quality.
6. Utilizing a pendulum-type viscoelastic measurement to enable determination of the interactions between the double layer ink and the pendulum fulcrum.

Acknowledgment. The author expresses his deepest appreciation to Mr. Yasuhiro Takeda, a former Senior Managing Director, and Mr. Tasuku Chiba, a former Director and General Manager in charge of the Business Division, for their kind guidance and assistance regarding the author's studies on this subject at Alps Electric Co., Ltd. The author also express many thanks to Mr. Shyuhei Takeuchi, a former Project Manager of the General Business Division, Mr. Kohsaki Yanata, a former Manager of the 2nd Engineering Department of the System Devices Division, as well as Mr. Takashi Shirakawa, Exective Engineer, Mr. Noboru Tsushima, Chief Engineer, Mr. Hiroshi Kobayashi, Mr. Yasutoshi Inoue, Mr. Kohsei Ohkami, Mr. Shinichi Sagawai, Mr. Hirotoshi Terao and other persons, for offering valuable opinions and suggestions to the author. The author appreciates the valuable assistance offered by Mr. Tadao Seto, a former Director of Fujicopian Co., Ltd. and other persons for the fabrication of the ink ribbons.

References

1. Y. Tokunaga, M. Yoshida and M.Takano, *Electronics and Telecommunications Society Technical Report*, IE-79-58 (1979).
2. Y. Tokunaga and K. Sugiyama, *IEEE Trans. Electron. Dev.* **ED-27,** 1, 218 (1980).
3. Y. Tokunaga and R. Takano, *J. Appl. Photgr. Eng.* **7,** 1, 10 (1981).
4. S. Ando, H. Taniguchi, H. Ogata, and K. Motoyama, *Proc. Image Electronics Society National Convention* **13,** 49–52 (1985).
5. K. Tsukaya and S. Ohta, *Pulp and Paper Technology Times*, 59–63 (Aug. 1987).
6. H. Sugiyama, S. Sakatoku, M. Matsumura, T. Kubota, and C. Hara, *Kobe Electric Technical Report* **37,** 63–69 (1992).
7. A. Uno, F. Igota, M. Ohkubo, K. Hatakeyama, and Y. Miyoshi, *NEC Technical Report* **46,** 51–55 (1993).
8. I. Hibino, *Electronics and Telecommunications Society Technical Report* **95,** (no. 507, EID95 94 – 98), 7–12 (1996).